

Channel Capacity and Bounds In Mixed Gaussian-Impulsive Noise

Tianfu Qi, *Graduate Student Member, IEEE*, Jun Wang, *Senior Member, IEEE*, Xiaoping Li, *Member, IEEE*

Abstract—¹Communication systems suffer from mixed noise consisting of both non-Gaussian impulsive noise (IN) and white Gaussian noise (WGN) in many practical applications. However, there is little literature about the channel capacity under mixed noise. In this paper, we first investigate statistical properties of the mixed noise model and demonstrate the existence and uniqueness of the capacity-achieving input distribution under the p -th moment constraint. Then, we derive lower and upper capacity bounds with closed expressions. It is shown that the lower bounds can degenerate to the well-known Shannon formula under special scenarios. More importantly, we obtain the convergence of the lower and upper bound and therefore, the asymptotic and analytical capacity expression is obtained. In addition, the capacity for specific modulations and the corresponding lower bounds are discussed. Numerical results reveal that the capacity decreases as the impulsiveness of the mixed noise becomes dominant and the proposed capacity bounds are very tight.

Index Terms—Mixed noise, channel capacity, capacity bound, relative entropy

I. INTRODUCTION

A. Related works

Characterized by an extremely short duration with large power, impulsive noise (IN) exists in many practical scenarios such as LTE in urban environments [1], wireless digital video broadcasting terrestrial (DVB-T), lightning, underwater acoustic systems [2], wide-band powerline communications [3], etc. The most popular model to describe IN is symmetric α stable (S α S) distribution which is discussed comprehensively in [4]. However, S α S distribution has no general closed-form probability density function (PDF). In practice, due to the Brownian motion of electrons, there always exists white Gaussian noise (WGN) in communication systems. Therefore, IN and WGN together generate mixed noise [5].

Capacity represents the ability to transfer error-free information between the communication transmitter and the receiver. The well-known channel capacity under WGN was proposed by Shannon [6]. Subsequently, the capacities of many other channels with different constraints have been analyzed. For instance, Abou-Faycal et al. systematically study the capacity of memoryless Rayleigh fading channels in [7] and give the amplitude's characteristic of the capacity-achieving input distribution. Hui Li et al. prove the existence and uniqueness

Tianfu Qi, Jun Wang are with the National Key Laboratory on Wireless Communications, University of Electronic Science and Technology of China, Chengdu 611731, China (e-mail: 202311220634@std.uestc.edu.cn).

Xiaoping Li is with the School of Mathematical Sciences, University of Electronic Science and Technology of China, Chengdu 611731, China (e-mail: lixiaoping.math@uestc.edu.cn).

¹The material in this paper was presented in part at the IEEE 98th Vehicular Technology Conference (VTC2023-Fall).

of capacity of the additive inverse Gaussian noise channel, and propose tight closed-form capacity bounds [8]. In [9], Lapidoth and Moser raise a general capacity upper bound by the dual expression of capacity, based on which numerical lower and upper bounds for several scenarios such as free-space optical intensity channel and Poisson channel are derived [10, 11]. The capacity of communication under S α S noise is calculated by the BA-algorithm [12] and its theoretical analysis is provided in [13]. However, the capacity of mixed noise channels is barely discussed in the existing literature.

Moreover, for power-limited communication systems, the modulation order cannot be infinite and there is a capacity limitation pertaining to the order. Thus, capacity under a specific modulation scheme is valuable for practical applications. Meilin He et al. present the capacity bounds of M-PAM modulation and the corresponding numerical calculation procedure [14] under WGN channel. However, there is no analytical or general capacity expression. In [15], the capacity of M-ary differential chaos shift keying modulation under WGN channel is analyzed, and explicit capacity bounds are provided. Pei Yang et al. develop a recurrence formula to construct the series representation as a numerically efficient way to obtain the capacity bound of Nakagami- m fading channel for BPSK and QPSK modulations [16].

B. Motivations

The existing works mainly focus on the pure impulsive noise described by α stable distribution or Middleton's class A (MCA) model. However, the WGN is ubiquitous in practical scenarios and therefore, we want to know whether or not there is an obvious influence of WGN on the analysis of channel capacity.

Sureka et al. propose an approximated PDF with the analytical form to describe the mixed noise consisting of WGN and IN which follows S α S distribution [17]. The derivation relies on the physical mechanism of mixed noise and therefore, it has been verified that the model can match the accurate distribution of mixed noise very well. We hope to solve the aforementioned problem with the aid of the approximated mixed noise model. In addition, based on the statistical properties of the model, we want to obtain analytical capacity bounds that are useful for practical applications. It is also expected that the bounds are general such that they can be applied for WGN and pure IN which are special cases of the mixed noise. To the best of the authors' knowledge, there is no reported work addressing all of above problems.

C. Contributions

The model of mixed noise channel is more complicated than that of IN including S α S distribution, Cauchy distribution, etc. In this paper, we analyze the capacity of mixed noise channel. Both general and special cases with respect to specific modulations are considered. The main contributions of this paper are summarized as follows:

- 1) First, the existence and uniqueness of channel capacity are discussed. We prove that the optimal input for the mixed noise channel exists and is unique based on the tightness of input distribution function set and the dominated convergence theorem.
- 2) Second, the closed-form lower and upper bounds of channel capacity are derived. By minimizing the KL divergence, we get an approximation of the mixed noise model. Then, we derive the lower and upper bounds of the capacity based on the mutual information and relative entropy, respectively. We analyze the generality and tightness of the proposed bounds and more importantly, obtain the analytical and asymptotic capacity expression.
- 3) Last but not least, the capacity with respect to PAM modulation is investigated. Based on the Hermite quadrature and Fano's inequality, we derive two lower capacity bounds. Numerical results show that these bounds are very tight.

D. Organizations

The remainder of this paper is organized as follows. In Section II, we provide the mixed noise model and derive important properties that will be utilized in the following analysis. In Section III, we formulate and analyze the capacity of mixed noise model with power constraints. Moreover, the existence and uniqueness of the capacity-achieving distribution are discussed. Analytical lower and upper bounds of the channel capacity and the asymptotic and closed-form capacity expression are obtained in section IV. In Section V, the capacity and bounds related to PAM modulation are considered. Numerical results and corresponding applications are described in Section VI. Finally, the paper is concluded in Section VII.

II. MIXED NOISE MODEL

We consider the communication problem under the memoryless additive mixed noise channel in this paper. The received signal model is as follows,

$$Y = X + N_m, \quad (1)$$

$$N_m = N_s + N_g, \quad (2)$$

where N_m , N_s and N_g represent the random variables (RVs) of the mixed noise, IN and WGN, respectively. N_s and N_g are mutually independent and Y and X are separately the received and transmitted signal. We omit the time index as the considered channel is memoryless.

The IN can be well described by the α stable distribution which is a heavy-tail distribution [18]. It can be denoted as $S(\alpha, \beta, \gamma, w)$, where α , β , γ and w are the characteristic

parameter, skewness parameter, scale parameter and position parameter, respectively. For convenience, we leverage $N_s \sim S(\alpha, \beta, \gamma, w)$ to represent that N_s follows α stable distribution. The PDF of α stable distribution does not admit general closed-form PDF, except Gaussian distribution for $\alpha = 2$ and Cauchy distribution for $\alpha = 1$ [18]. Under communication scenarios, the IN is usually distributed symmetrically about zero, i.e., $\beta = w = 0$. Due to the lack of a simple PDF of S α S distribution, it is more difficult to model the mixed noise. Sureka *et al.* propose an approximated model for mixed noise and its PDF is shown as follows [17],

$$f_{N_m}(n) = \frac{g_0}{I} \left[c_1 e^{-\frac{n^2}{4\gamma_{sg}}} + \frac{c_2(1-c_1)}{|n|^{\alpha+1} + c_2} \right], \quad (3)$$

where

$$c_2 = \frac{\alpha\gamma_s C_\alpha}{g_0(1-c_1)}, \quad (4)$$

$$g_0 = \frac{1}{\pi} \sqrt{\frac{2^{-\frac{1}{2}-\frac{1}{\alpha}} \sqrt{\pi}}{\alpha \left(\gamma_s^{\frac{2}{\alpha}} + \gamma_g \right)}} \Gamma \left(\frac{1}{\alpha} \right), \quad (5)$$

$$C_\alpha = \frac{1}{\pi} \Gamma(\alpha) \sin \left(\frac{\alpha\pi}{2} \right), \quad (6)$$

$$I = 2c_1 g_0 \sqrt{\pi \gamma_{sg}} + 2g_0(1-c_1) c_2^{\frac{1}{\alpha+1}} \times \Gamma \left(\frac{\alpha}{\alpha+1} \right) \Gamma \left(\frac{\alpha+2}{\alpha+1} \right), \quad (7)$$

and $\Gamma(a) = \int_0^{+\infty} t^{a-1} e^{-t} dt$. The distribution includes 5 parameters which are $0 < \alpha \leq 2$, $\gamma_s > 0$, $\gamma_g > 0$, $0 \leq c_1 \leq 1$ and $\gamma_{sg} > 0$. α is the characteristic parameter describing the thickness of the tail of the distribution, which is the identical parameter used in S α S distribution. γ_g and γ_s are the scale parameters of WGN and IN, respectively. c_1 can be considered as a weight factor, and the distribution will degenerate to Gaussian distribution when $c_1 = 1$. γ_{sg} is a regulatory factor for the main lobe of this distribution.

Subsequently, we give some important properties of the mixed noise model which will be utilized in what follows.

Property 1: $f_{N_m}(n)$ is continuous and $f_{N_m}(n) \leq g_0/I$.

This property is straightforward because of the monotonicity of the PDF. Before proceeding, we first provide an elementary integral formula [19],

$$\int \frac{x^r}{c+x^a} dx = \frac{x^{r+1}}{c(r+1)} {}_2F_1 \left(1, \frac{r+1}{a}; \frac{a+r+1}{a}; -\frac{x^a}{c} \right), \quad (8)$$

where ${}_2F_1(\cdot, \cdot; \cdot; \cdot)$ is the Gaussian hypergeometric function. Furthermore, the following linear transform equation is used to deduce the limit of the integral (8) [19],

$$\begin{aligned} & {}_2F_1(a, b; c; z) \\ &= \frac{\Gamma(c)\Gamma(b-a)}{\Gamma(b)\Gamma(c-a)} (-z)^{-a} {}_2F_1 \left(a, a+1-c; a+1-b; \frac{1}{z} \right) \\ &+ \frac{\Gamma(c)\Gamma(a-b)}{\Gamma(a)\Gamma(c-b)} (-z)^{-b} {}_2F_1 \left(b, b+1-c; b+1-a; \frac{1}{z} \right). \end{aligned} \quad (9)$$

Consequently,

$$\int_0^{+\infty} \frac{x^r}{c+x^\alpha} dx = \frac{c^{\frac{r-\alpha+1}{\alpha}}}{r+1} \Gamma\left(1 + \frac{r+1}{\alpha}\right) \Gamma\left(\frac{\alpha-r-1}{\alpha}\right)$$

with ${}_2F_1(a, b; c; 0) = 0$ and $r+1 < a$. Then, the moment of the mixed noise is provided by the following property.

Property 2: $f_{N_m}(n)$ has no limited variance. It has finite p -th moment ($p < \alpha \leq 2$) which can be expressed as

$$\begin{aligned} \mathbb{E}[|N_m|^p] &= \frac{c_1 g_0}{I} (2\gamma_{sg})^{p+1} \Gamma\left(\frac{p+1}{2}\right) \\ &\quad + \frac{2(1-c_1)g_0 c_2^{\frac{p+1}{\alpha+1}}}{(p+1)I} \Gamma\left(1 + \frac{p+1}{\alpha+1}\right) \Gamma\left(\frac{\alpha-p}{\alpha+1}\right). \end{aligned} \quad (10)$$

Property 3: When the mixed noise degenerates to Gaussian noise, we have

$$\alpha = 2, c_1 = 1, c_2 = +\infty, C_\alpha = 0, I = 2g_0\sqrt{\pi\gamma_{sg}}. \quad (11)$$

Then, the model (3) can be simplified as

$$f_{N_m}(n) = \frac{1}{2\sqrt{\pi\gamma_{sg}}} e^{-\frac{n^2}{4\gamma_{sg}}}. \quad (12)$$

Similarly, when the mixed noise degrades to pure impulsive noise, we have the following property.

Property 4: When the mixed noise degenerates to impulsive noise, the model (3) can be simplified as

$$f_{N_m}(n) = \frac{\alpha\gamma_s C_\alpha}{I(|n|^{\alpha+1} + c_2)}, \quad (13)$$

and

$$\begin{aligned} c_1 &= 0, c_2 = \frac{\alpha\gamma_s C_\alpha}{g_0}, \\ I &= 2g_0 c_2^{\frac{1}{\alpha+1}} \Gamma\left(\frac{\alpha}{\alpha+1}\right) \Gamma\left(\frac{\alpha+2}{\alpha+1}\right). \end{aligned} \quad (14)$$

From the property 3 and 4, it can be observed that c_1 represents the ratio of WGN and IN. Different choices of c_1 lead to a significant influence on the statistical property of the mixed noise.

Property 5: $f_{N_m}(n) = \mathcal{O}(n^{-\alpha+\eta-1})$ where $\mathcal{O}(\cdot)$ represents the upper bounded function. That is, $\exists N > 0, \alpha > \eta > 0, k > 0, \forall n > N$, we have

$$f_{N_m}(n) \leq \frac{k}{n^{\alpha-\eta+1}}. \quad (15)$$

Property 6: $f_{N_m}(n) = \omega(n^{-\alpha-\delta-1})$ where $\omega(\cdot)$ represents the lower bounded function. That is, $\exists N > 0, \delta > 0, k > 0, \forall n > N$, we have

$$f_{N_m}(n) \geq \frac{k}{n^{\alpha+\delta+1}}. \quad (16)$$

Property 5 and 6 can be proved straightforwardly since the main lobe of PDF (3) decays extremely fast and all the parameters of the tail section are finite.

Remarks: Comparing with existing noise models, it is worth noting that the mixed noise model (3) is more general. The underlying reasons are as follows,

- 1) The non-Gaussian IN exists in various scenarios [1–3], where the WGN inevitably exists due to the Brownian

movement of electrons. The resulting mixed noise can be well described by (3). Meanwhile, The model can degenerate to special cases with specific parameters as described in property 3 and 4. Hence, the model is able to describe a class of noise, including WGN, IN and mixed Gaussian-impulsive noise (MGIN).

- 2) In contrast to SoS distribution, the mixed noise model has a concise and closed-form PDF, which facilitates performance analysis. Specifically, it can be utilized to derive analytical capacity bounds. Moreover, the capacity bounds with respect to specific modulation schemes can also be obtained for practical applications.

III. EXISTENCE AND UNIQUENESS OF OPTIMAL INPUT DISTRIBUTING

For the MGIN channel, it is rather challenging to obtain explicit channel capacity due to the complicated PDF expression, the lack of the second moment, etc. In this section, we first formulate the optimization problem with power constraints. Then, we analyze the existence and uniqueness of the capacity-achieving input distribution as the theoretical foundation of the following analysis.

A. Problem formulation and settings

Let $F_X(\cdot)$ denote the cumulative density function (CDF) of X . To conveniently express the distribution function F_X of X , we define $\mathcal{B}(\mathbb{R})$ to be the Borel σ -algebra generated by \mathbb{R} . Denote the probability measure of X by μ_X which admits support \mathbb{R} and is defined on $(\mathbb{R}, \mathcal{B}(\mathbb{R}))$. We set the power constraint of X to be

$$\mathbb{E}_{\mu_X}[|X|^p] \leq P_0 < +\infty, 1 \leq p < \alpha \leq 2. \quad (17)$$

In (17), the lower bound of p is to ensure the constraint is convex. Here, we do not apply the variance as the power constraint since the p -th norm is more general and weaker. In other words, if X has a finite variance, it admits finite p -th moment but not vice versa. Meanwhile, from the perspective of functional equivalence, the p -th norm ($0 < p < +\infty$) (17) can also describe the power of input. Without loss of generality, we consider the distribution of X to be symmetric, that is,

$$F_X(x) = 1 - F_X(-x), \forall x \geq 0. \quad (18)$$

(18) is reasonable since the direct current offset can be eliminated by subtracting a constant from the received signals. Thus, it is obvious that the output distribution $F_Y(y)$ should be symmetric. Then, the feasible set Ω of input distribution functions is

$$\Omega = \left\{ F_X : \mathbb{E}_{\mu_X}[|x|^p] \leq P_0, F_X(x) = 1 - F_X(-x), \forall x \in \mathbb{R}, 1 \leq p < \alpha \leq 2 \right\}. \quad (19)$$

Therefore, the capacity can be expressed as

$$C = \sup_{F_X \in \Omega} I(F_X) = \sup_{F_X \in \Omega} \{h(Y) - h(Y|X)\}, \quad (20)$$

where ' $I(\cdot)$ ' and ' $h(\cdot)$ ' denote mutual information and entropy, respectively. For the sake of simplicity, we apply $I(F_X)$

instead of $I(X;Y)$ since it is only related to F_X when the channel model is fixed.

Note that it can be proved that $h(Y)$ and $h(Y|X)$ are both always finite based on Gibbs's inequality and the following lemma. We omit the proof since it is well-known.

Lemma 1: $\mathbb{E}_{\mu_Y}[|Y|^p]$ is finite for any $p < \alpha$.

Proof: According to Minkowski's inequality, we have

$$\begin{aligned} \mathbb{E}_{\mu_Y}[|Y|^p]^{\frac{1}{p}} &\leq \mathbb{E}_{\mu_X}[|X|^p]^{\frac{1}{p}} + \mathbb{E}_{\mu_{N_m}}[|N_m|^p]^{\frac{1}{p}} \\ &\leq P_0^{\frac{1}{p}} + \mathbb{E}_{\mu_{N_m}}[|N_m|^p]^{\frac{1}{p}} < +\infty. \end{aligned} \quad (21)$$

For the second inequality, the first term is due to the power constraint of the input distribution, and the second one is from the property 2. ■

The lemma 1 will also be leveraged in derivations of the bounds of the capacity. Then, we discuss the existence and uniqueness of optimal input distribution and present the characteristics of the capacity-achieving distribution.

B. Existence and Uniqueness

According to optimization theory, if the Ω is weak* compact and the mutual information function is weak* continuous, the existence can be concluded. Furthermore, if Ω is also convex and $I(F_X)$ is a strictly concave function in Ω , capacity-achieving input will be unique [20].

In general, the convexity can be verified by its definition if the power constraint is convex. Then, the compactness can be proved by utilizing Prokhorov's theorem as shown in [7] and the key point is to show that Ω is tight. Subsequently, the weak continuity is demonstrated by the dominated convergence theorem and the key point is to build the dominate function. In fact, the continuity of $h(N_m)$ is obvious based on the PDF and we just need to show $h(Y)$ is also weak* continuous. Finally, the uniqueness of channel capacity can be proved by the Levy continuity theorem. **Consequently, to avoid redundancy, we will prove the tightness of Ω and construct the dominated function for $f_Y(y) \log f_Y(y)$.**

Proposition 1: Ω is tight.

Proof: To show the tightness of Ω , it is equivalent that $\forall \epsilon > 0$, there $\exists L > 0$ such that [7]

$$\sup_{F_X \in \Omega} 1 - F_X(L) < \epsilon, \quad (22)$$

Indeed, $\mathbb{E}[|X|^p]$ is finite and we have

$$\begin{aligned} \mathbb{E}[|X|^p] &= 2 \left[\int_0^L |x|^p f_X(x) dx + \int_L^{+\infty} |x|^p f_X(x) dx \right] \\ &\geq 2(M + L^p[1 - F(L)]), \end{aligned} \quad (23)$$

where $M \triangleq \int_0^L |x|^p f_X(x) dx$. Therefore, we can get

$$0 < 1 - F(L) \leq \frac{\mathbb{E}[|X|^p] - 2M}{2L^p} \leq \frac{P_0 - 2M}{2L^p}. \quad (24)$$

Then, we need an upper bound with the analytic expression of $-M$, which is equivalent to finding an upper bound for $\int_L^{+\infty} |x|^p f_X(x) dx$. Actually, for any $L_t > 0$,

$$\int_{L_t}^{+\infty} |x|^p f_X(x) dx < \frac{P_0}{2}. \quad (25)$$

Based on the power constraint, it can be seen that the decay order of $f_X(x)$ should be larger than $p + 1$, i.e., $f_X(x) = \mathcal{O}(|x|^{-p-1})$. We assume that there exists a finite L_t such that $f_X(x) \leq k/x^{p+r+1}$, $r > 0$ if $x \geq L_t$. Combing with (25), we can get that $k \leq P_0 r L_t^r / 2$. Therefore,

$$\begin{aligned} \int_L^{+\infty} |x|^p f_X(x) dx &\leq \int_L^{+\infty} |x|^p \frac{P_0 r L_t^r}{2x^{p+1+r}} dx \\ &= \frac{P_0 L_t^r}{2L^r}, \quad L \geq L_t. \end{aligned} \quad (26)$$

In this way,

$$\begin{aligned} -M &= - \left[\frac{P_0}{2} - \int_L^{+\infty} |x|^p f_X(x) dx \right] \\ &\leq \frac{P_0}{2} \left(\frac{L_t^r}{L^r} - 1 \right), \end{aligned} \quad (27)$$

$$\frac{P_0 - 2M}{2L^p} \leq \frac{P_0 L_t^r}{2L^{r+p}} < \epsilon. \quad (28)$$

Let $L \geq \max\{L_t, (P_0 L_t^r / 2\epsilon)^{1/(r+p)}\}$ and then, we can conclude Ω is tight. ■

Before introducing the dominated function, we first present the following lemma.

Lemma 2: $|x \log x| < \frac{2}{1-r} x^r$, $0 < x < 1$, $0 < r < 1$.

Proof: When $0 < x < 1$, $|x \log x| = -x \log x$. We define function $g(x) = 2x^r/(1-r) + x \log x$. It can be verified that $g(x)$ is convex when $x \in (0, 1)$. Consequently, the minimum of $g(x)$ can be obtained to be $\min\{g(x)\} = 2x^{r-1} - 1 > 0$ via $\frac{\partial g(x)}{\partial x} = 0$. ■

Proposition 2: There exists a dominated function which is absolute integrable for $f_Y(y) \log f_Y(y)$.

Proof: The PDF of received signal $f_Y(y)$ can be expressed as

$$f_Y(y) = \int_{-\infty}^{+\infty} f_{N_m}(y|x) dF_X. \quad (29)$$

It follows (3) that $f_Y(y) < g_0/I$. Based on (17), we have

$$\int_{-\infty}^{+\infty} |x|^p f_X(x) dx \leq P_0 < +\infty. \quad (30)$$

Taking into account property 5 and the decay order of f_X jointly, we have

$$\begin{aligned} f_Y(y) &= 2 \left[\int_0^y f_{N_m}(y|x) dF_X + \int_y^{+\infty} f_{N_m}(y|x) dF_X \right] \\ &\leq 2 \left[\int_0^y \frac{k_2}{y^{\alpha+1-\eta}} dF_X + \frac{g_0}{I} \int_y^{+\infty} dF_X \right] \\ &\leq 2 \left[\frac{k_2}{y^{\alpha+1-\eta}} \int_{-\infty}^{+\infty} dF_X + \frac{g_0}{I} \int_y^{+\infty} \frac{k_1}{x^{p+1}} dx \right] \\ &= \frac{2k_2}{y^{\alpha+1-\eta}} + \frac{2g_0 k_1}{y^p I p} \triangleq \mathcal{G}(y), \quad y > y_t, \end{aligned} \quad (31)$$

where $\alpha > \eta$ and we assume y_t satisfying $\mathcal{G}(y_t) = \frac{1}{2}$. Furthermore, we define $\chi_{Y|Y}(y)$ to be

$$\chi_{Y|Y}(y) = \begin{cases} \frac{g_0}{I}, & 0 \leq y < x_0 \\ \max \left\{ \frac{4k_2}{y^{\alpha+1-\eta}}, \frac{4g_0 k_1}{y^p I p} \right\} \leq 1, & y \geq y_t. \end{cases} \quad (32)$$

Note that the $\chi_Y(y), y \geq y_t$ should be less than 1 to satisfy the domain of the function in proposition 2. Therefore, based on the proposition 2, the dominated function of $|f_Y(y) \log f_Y(y)|$ can be

$$\chi(y) = \begin{cases} \frac{g_0}{I} \log \frac{g_0}{I}, & 0 \leq y < x_0 \\ \frac{2}{1-r} \max \left\{ \left(\frac{4k_2}{y^{\alpha+1-\eta}} \right)^r, \left(\frac{4g_0k_1}{y^p I p} \right)^r \right\}, & y \geq y_t. \end{cases} \quad (33)$$

Obviously, when we choose $\max \{r(\alpha+1-\eta), rp\} > 1$, $\chi(y)$ is still absolutely integrable along the real number line and then, the dominated function can be established. ■

Finally, with the proposition 1 and 2, both existences and uniqueness can be concluded.

C. Characteristics of Capacity-achieving Input Distribution

In the previous subsection, we know that the optimal input for the MGIN channel exists and is unique. Subsequently, we discuss the characteristics pertaining to capacity-achieving input distribution via the KKT conditions which will be used to calculate the capacity numerically. As the derivation procedure is well-known, we only briefly provide the results for completeness.

By taking constraint (17) into consideration, the Lagrange function of mutual information is

$$J(F_X, \lambda) = I(F_X) - \lambda \underbrace{\left(\int_{-\infty}^{+\infty} |x|^p dF_X - P_0 \right)}_{\phi(F_X)}, \quad (34)$$

where λ is a non-negative Lagrangian multiplier. Note that $\phi(F_X)$ is a convex constraint due to $p \geq 1$. Meanwhile, the symmetry constraint is not integrated into (34) as F_X is symmetric by default. Moreover, we can only consider the amplitude of X .

As it has been proved that Ω is a convex set and $I(F_X)$ is concave, the Lagrangian theorem is satisfied. Furthermore, it always holds that $\frac{\partial J(F_X, \lambda)}{\partial F_X} \leq 0$ for $\forall F_X \in \Omega$ and $I(F_X)$ can reach the maximum in Ω at F_X^* and $\frac{\partial J(F_X, \lambda)}{\partial F_X} \Big|_{F_X=F_X^*} = 0$ if $I(F_X)$ and $\phi(F_X)$ are weakly differentiable, which can be easily verified.

Consequently, with (34) and some manipulations, we have the following inequality,

$$\begin{aligned} \frac{\partial J(F_X, \lambda)}{\partial F_X} &= -\mathbb{E}_{\mu_X} \left[\int_{-\infty}^{+\infty} f_{N_m}(y|x) \log f_Y(y, F_X^*) dy \right] - C \\ &\quad + h(N_m) - \lambda[\phi(F_X) - \phi(F_X^*)] \leq 0, \forall F_X \in \Omega. \end{aligned} \quad (35)$$

Based on theorem 4 in [7], (35) can be equivalently transformed into

$$\begin{aligned} K(x, \lambda) &= \int_{-\infty}^{+\infty} f_{N_m}(y|x) \log f_Y(y, F_X^*) dy + C - h(N_m) \\ &\quad + \lambda(|x|^p - P_0) \begin{cases} > 0, & \forall x \in \mathbb{R} - \mathcal{S}^* \\ = 0, & \forall x \in \mathcal{S}^*, \end{cases} \end{aligned} \quad (36)$$

where \mathcal{S}^* indicates the set containing optimal mass points. Actually, the points in \mathcal{S}^* are the mass points of F_X^* in Ω

and they are completely related. (36) reveals that for given F_X^* , there exists $\lambda > 0$ such that the equality holds if $x \in \mathcal{S}^*$. Furthermore, the Slater's constraint qualification can be satisfied by F_X , which assures F_X^* is optimal if there are Lagrange multipliers satisfying KKT conditions.

Then, based on the similar procedures in [7] and [21], it can also be shown that the optimal input distribution is discrete and only contains finite mass points by contradiction. We omit the derivation to avoid the repetitions.

IV. LOWER AND UPPER BOUNDS OF CAPACITY

The channel capacity can be computed based on numerical methods, e.g., Blahut-Arimoto (BA) algorithm. However, it is preferable to obtain the capacity bounds with analytical expressions. In this section, we first derive the closed-form capacity lower bounds based on the mutual information. Subsequently, the upper bound based on the duality expression of capacity is obtained. Finally, the generality and asymptotic behaviors of lower and upper bounds are discussed.

Before proceedings, we propose the model approximation method which will be utilized in what follows.

Theorem 1: The mixed noise model in (3) can be approximated as follows,

$$f_{N_m}(n) \approx \hat{f}_{N_m}(n) = \begin{cases} \frac{g_0}{I} e^{-\frac{n^2}{4\gamma_{sg}}}, & |n| < n_0 \\ \frac{\alpha\gamma_s C_\alpha}{I(|n|^{\alpha+1} + c_2)}, & |n| \geq n_0, \end{cases} \quad (37)$$

where n_0 is the intersection of piecewise functions in (37) under Kullback-Leibler divergence (KLD) minimization criteria.

Proof: We first explain the motivation to approximate the noise model (3). As the mixed noise model (3) is the linear combination of two functions, it is extremely challenging to obtain closed-form mutual information due to the log operation. Nevertheless, when n becomes large, the influence of the exponential term can be neglected. Moreover, we can observe that the two piecewise functions in (3) have similar behaviors when $|n| < n_0$, i.e., $e^{-\frac{n^2}{4\gamma_{sg}}} \approx \frac{c_2}{|n|^{\alpha+1} + c_2}$. Therefore, we can only retain the exponential term to approximate the whole PDF when $|n| < n_0$. Thus, (37) can be obtained, and the remaining task is to determine n_0 .

As KLD can measure the difference between two distribution functions [17], we determine n_0 by minimizing the KLD between $f_{N_m}(n)$ and $\hat{f}_{N_m}(n)$, which is written as

$$\begin{aligned} &\frac{1}{2} \mathcal{K} \left(f_{N_m}(n); \hat{f}_{N_m}(n) \right) \\ &= \int_0^{+\infty} f_{N_m}(n) \log \frac{f_{N_m}(n)}{\hat{f}_{N_m}(n)} dn \\ &= \int_0^{+\infty} f_{N_m}(n) \log f_{N_m}(n) dn - \log \frac{g_0}{I} \int_0^{n_0} f_{N_m}(n) dn \\ &\quad + \frac{1}{4\gamma_{sg}} \int_0^{n_0} n^2 f_{N_m}(n) dn + \int_{n_0}^{+\infty} f_{N_m}(n) \log \frac{I}{\alpha\gamma_s C_\alpha} dn \\ &\quad + \int_{n_0}^{+\infty} f_{N_m}(n) \log (|n|^{\alpha+1} + c_2) dn. \end{aligned} \quad (38)$$

As $f_{N_m}(n)$ and $\hat{f}_{N_m}(n)$ are both symmetric, we only consider the non-negative part. For example,

$$\begin{aligned} \frac{\partial \mathcal{K}}{\partial n_0} = & \left(-\log \frac{g_0}{I} + \frac{n_0^2}{4\gamma_{sg}} \right) f_{N_m}(n_0) - \left[\log(|n_0|^{\alpha+1} \right. \\ & \left. + c_2) + \log \frac{g_0}{\alpha\gamma_s C_\alpha} \right] f_{N_m}(n_0). \end{aligned} \quad (39)$$

By setting it to zero, we can get

$$\frac{\partial \mathcal{K}}{\partial n_0} = 0 \Rightarrow \frac{\alpha\gamma_s C_\alpha}{g_0 (|n_0|^{\alpha+1} + c_2)} = e^{-\frac{n_0^2}{4\gamma_{sg}}}. \quad (40)$$

The optimal n_0 can then be determined by solving the above equation numerically. \blacksquare

In accordance with theorem 1, $h(N_m)$ can be analytically computed. Moreover, the theorem 1 also assures that the approximated noise model is still continuous.

A. Lower Bound

In this subsection, we find a capacity lower bound based on the mutual information. We set $f_X(x)$ to be a distribution so that the resulting $f_Y(y)$ can be easily handled.

1) *The input with the same distribution as the channel noise:* For the WGN channel, the optimal input distribution with power constraint is also Gaussian distributed. In fact, the non-Gaussian impulsive noise follows the stable distribution which retains many of the same properties of the Gaussian distribution. For example, the summation of stable R.V.s is still stable. Thus, motivated by the Gaussian channel case, let X follow the same distribution with N_m , i.e., the distribution of X is given as follows,

$$f_X(x) = \frac{g_{x0}}{I_x} \left[c_{x1} e^{-\frac{x^2}{4\gamma_{xsg}}} + \frac{c_{x2}(1 - c_{x1})}{|x|^{\alpha+1} + c_{x2}} \right], \quad (41)$$

where the additional subscript x is added in these parameters to avoid notational confusion. The similar operation is also applied in what follows. Then, we will show that Y has the same distribution as N_m . According to (2), X and Y can be expressed as

$$X = X_g + X_s, \quad (42)$$

$$Y = Y_g + Y_s = (X_g + N_g) + (X_s + N_s), \quad (43)$$

where both X_g and N_g follow Gaussian distribution, and both X_s and N_s follow α stable distribution, i.e., $X_g \sim \mathcal{N}(0, 2\gamma_{xg}^2)$, $N_g \sim \mathcal{N}(0, 2\gamma_{ng}^2)$, $X_s \sim S(\alpha, 0, \gamma_{xs}, 0)$ and $N_s \sim S(\alpha, 0, \gamma_{ns}, 0)$. Based on the additive property of Gaussian distribution and SoS distribution [18], we can get $Y_g \sim \mathcal{N}(0, 2\gamma_{yg}^2)$ and $Y_s \sim S(\alpha, 0, \gamma_{ys}, 0)$. Then we can conclude Y also follows the mixed noise model with $\gamma_{yg} = (\gamma_{xg}^2 + \gamma_{ng}^2)^{1/2}$ and $\gamma_{ys} = (\gamma_{xs}^\alpha + \gamma_{ns}^\alpha)^{1/\alpha}$. c_{y1} and γ_{ysg} can be estimated based on the empirical methods presented in [17].

Finally, it follows mutual information and theorem 1 that the lower bound can be given as

$$C \geq h(Y) - h(N_m) \triangleq L_1. \quad (44)$$

The detailed derivation and analytical expressions can be found in Appendix A.

2) *Input based on the maximum entropy theorem:* The lower bound L_1 is a little heuristic and we want to find a simpler bound with more theoretical foundations. Here, we further present a closed-form lower bound in accordance with the entropy power inequality [6], which can be expressed as follows,

$$C \geq \frac{1}{2} \log \left(1 + e^{2[h(X) - h(N_m)]} \right) \triangleq L_2. \quad (45)$$

Thus, we can get a tighter lower bound by maximizing $h(X)$ with the constraint (17) and (18). According to the maximum entropy theorem, the optimal $f_X(x)$ should be

$$f_X(x) = e^{\lambda_0 + \lambda_1 |x|^p}, \forall x \in \mathbb{R}. \quad (46)$$

Meanwhile, $f_X(x)$ should satisfy

$$\int_{-\infty}^{+\infty} f_X(x) dx = 1, \quad (47)$$

$$\int_{-\infty}^{+\infty} |x|^p f_X(x) dx = P_0. \quad (48)$$

Then, we can solve that

$$\lambda_0 = \frac{p-1}{p} \log p - \frac{1}{p} \log P_0 - \log [2\Gamma(1/p)], \quad (49)$$

$$\lambda_1 = -\frac{1}{pP_0}, \quad (50)$$

$$h(X) = -\lambda_0 + \frac{1}{p}. \quad (51)$$

Therefore, the capacity lower bound can be obtained as

$$L_2 = \frac{1}{2} \log \left(1 + e^{2[-\lambda_0 + 1/p - h(N_m)]} \right). \quad (52)$$

Note that $h(N_m)$ has been calculated in Appendix A.

Remarks: In the next subsection, we will see that the equality of the entropy power inequality can be achieved and the corresponding lower bound will converge to the channel capacity as the signal power continues to increase.

3) *Asymptotical behaviors and generality:* When the mixed noise channel is very close to Gaussian channel, the parameters of the mixed noise model follow property 3. Therefore, we have

$$\begin{aligned} \lim_{c_{y1} \rightarrow 1} h(Y) = & -\frac{g_{y0}}{I_y} \left\{ y_0 e^{-\frac{y_0^2}{4\gamma_{ysg}}} + \left(2 \log \frac{g_{y0}}{I_y} - 1 \right) \sqrt{\pi \gamma_{ysg}} \right. \\ & \left. \times \left[1 - 2\mathcal{Q} \left(\frac{y_0}{\sqrt{2\gamma_{ysg}}} \right) \right] \right\}, \end{aligned} \quad (53)$$

where $\mathcal{Q}(z) = \frac{1}{\sqrt{2\pi}} \int_z^{+\infty} e^{-t^2} dt$. Recall the definition of y_0 , it can be concluded that $\lim_{c_{y1} \rightarrow 1} y_0 = +\infty$ since the tail section becomes zero and the intersection will be reached when $y \rightarrow +\infty$. In this way,

$$\begin{aligned} \lim_{c_{y1} \rightarrow 1} h(Y) = & -\frac{g_{y0}}{I_y} \sqrt{\pi \gamma_{ysg}} \left(2 \log \frac{g_{y0}}{I_y} - 1 \right) \\ = & \frac{1}{2} \log 4\pi e \gamma_{ysg}. \end{aligned} \quad (54)$$

Therefore, the bound (44) becomes

$$C \geq \frac{1}{2} \log \frac{\gamma_{ysg}}{\gamma_{nsq}}, \quad (55)$$

where γ_{ysg} denotes the variance and is additive, i.e., $\gamma_{ysg} = \gamma_{nsg} + \gamma_{xsg}$. Then, (55) could be $C \geq \frac{1}{2} \log(1 + \gamma_{xsg}/\gamma_{nsg}) = \frac{1}{2} \log(1 + P_X/P_N)$. In this case, p can be set to 2 since the finite variance exists, and the bound will be certainly Shannon capacity. In fact, the equality is reached because the optimal input is Gaussian distributed.

As for L_2 , when MGIN turns to WGN and p converges to 2, the distribution will be Gaussian distribution. Then, Y is also a Gaussian RV and L_2 will degenerate to Shannon formula. The analysis indicates the generality of the two lower bounds. Note that when MGIN degenerates to IN, the approximation of (44) will introduce a large error and y_0 will converge to 0. However, the similar capacity lower bounds can be calculated directly based on property 4. The derivation is similar to the Appendix A and therefore, we omit it in this paper.

B. Upper bound

In [9], the discrete duality inequality based on relative entropy was provided and it was extended to continuous form which is equivalent to an infinite input alphabet. The generalized upper bound is expressed as

$$C \leq \mathbb{E}_{\mu_X} [\mathcal{K}(f_{N_m}(y|x); f_R(y))], \quad (56)$$

where $f_R(y)$ is an arbitrary output distribution to generate the upper bound. The equality is achieved when $f_R(y) = f_Y(y)$ and $f_Y(y)$ is the output PDF corresponding to the optimal input. An elaborated $f_R(y)$ will lead to a tight upper bound with closed form. For convenience, we still utilize the parameters in (37) to represent the distribution of N_m in the following.

1) *Output based on the dual optimization problem:* The channel capacity is formulated by the optimization problem to find the best input distribution. However, the second term of (20) is independent of the input and thus, the problem can be reformulated as

$$\begin{aligned} C &= \sup_{F_X \in \Omega} \{h(Y) - h(Y|X)\} \\ &= \sup_{F_X \in \Omega} \{h(Y)\} - h(N_m) \\ &= \sup_{F_Y \in \tilde{\Omega}} \{h(Y)\} - h(N_m). \end{aligned} \quad (57)$$

Thus, the optimized problem (20) is converted to its duality which is to determine the best output distribution with corresponding constraints. Consider (17) and (18), there is also the power constraint for Y . Unfortunately, the accurate power constraint for Y cannot be obtained except for $p = 2$ which is also the Gaussian case. However, according to the lemma 1, the p -th moment of output is also finite. Furthermore, any r -th moment of Y with $r \leq p$ is also finite based on the Lyapunov inequality. Hence, feasible set $\tilde{\Omega}$ for F_Y is

$$\tilde{\Omega} = \left\{ F_Y : \mathbb{E}_{\mu_Y} [|Y|^r] \leq P_Y \leq +\infty, F_Y(y) = 1 - F_Y(-y), \forall y \in \mathbb{R}, 1 \leq p < \alpha \leq 2 \right\}. \quad (58)$$

Note that P_Y is unknown. In this way, the solution of the problem (57) is the same as that in the derivation of the lower bound L_2 . The above analysis motivates us to set the suitable

distribution for $f_R(\cdot)$ in (56) and the following theorem is obtained.

Theorem 2: Let the arbitrary output distribution $f_R(y)$ to be

$$f_R(y) = \frac{p}{2\Gamma(1/p)} \sigma_1^{-\frac{1}{p}} e^{-\frac{|y|^p}{\sigma_1}}, \forall y \in \mathbb{R}, \sigma_1 > 0, \quad (59)$$

where σ_1 is the parameter of $f_R(y)$. Then, the capacity upper bound is

$$\begin{aligned} C &\leq -\log \frac{p}{2\Gamma(1/p)} + \log \left(P_0^{\frac{1}{p}} + \mathbb{E}_{\mu_{N_m}} [|N_m|^p]^{\frac{1}{p}} \right) \\ &\quad + \frac{1}{p} + \frac{1}{p} \log p - h(N_m) \triangleq U. \end{aligned} \quad (60)$$

Proof: Based on (56), we can obtain that

$$\begin{aligned} C &\leq \inf_{\sigma_1} \{ \mathbb{E}_{\mu_X} [\mathcal{K}(f_{N_m}(y|x); f_R(y))] \} \\ &= \inf_{\sigma_1} \left\{ -\mathbb{E}_{\mu_X} \left[\int_{-\infty}^{+\infty} f_{N_m}(y|x) \log f_R(y) dy \right] - h(N_m) \right\}. \end{aligned} \quad (61)$$

Plugging (59) into (61) yields

$$\begin{aligned} &-\mathbb{E}_{\mu_X} \left[\int_{-\infty}^{+\infty} f_{N_m}(y|x) \log f_R(y) dy \right] \\ &= -\mathbb{E}_{\mu_X} \left[\int_{-\infty}^{+\infty} f_{N_m}(y|x) \left(\log \tilde{K}_1 - \frac{|y|^p}{\sigma_1} \right) dy \right] \\ &= -\log \left[\frac{p}{2\Gamma(1/p)} \sigma_1^{-\frac{1}{p}} \right] + \frac{\mathbb{E}_{\mu_X} \left[\int_{-\infty}^{+\infty} f_{N_m}(n) |x+n|^p dn \right]}{\sigma_1}. \end{aligned} \quad (62)$$

Then, according to Minkovski's inequality,

$$\begin{aligned} &\mathbb{E}_{\mu_X} \left[\int_{-\infty}^{+\infty} f_{N_m}(n) |x+n|^p dn \right] \\ &= \mathbb{E}_{\mu_X} [\mathbb{E}_{\mu_{N_m}} [|X+N_m|^p]] \\ &\leq \mathbb{E}_{\mu_X} \left[\left(\mathbb{E}_{\mu_{N_m}} [|X|^p]^{\frac{1}{p}} + \mathbb{E}_{\mu_{N_m}} [|N_m|^p]^{\frac{1}{p}} \right)^p \right]. \end{aligned} \quad (63)$$

Since X is independent of N_m , we have $\mathbb{E}_{\mu_{N_m}} [|X|^p]^{\frac{1}{p}} = |X|$. In this way,

$$\begin{aligned} &\mathbb{E}_{\mu_X} \left[\int_{-\infty}^{+\infty} f_{N_m}(n) |x+n|^p dn \right] \\ &\leq \mathbb{E}_{\mu_X} \left[\left(|X| + \mathbb{E}_{\mu_{N_m}} [|N_m|^p]^{\frac{1}{p}} \right)^p \right] \\ &\leq \left(\mathbb{E}_{\mu_X} [|X|^p]^{\frac{1}{p}} + \mathbb{E}_{\mu_X} [\mathbb{E}_{\mu_{N_m}} [|N_m|^p]]^{\frac{1}{p}} \right)^p \\ &\leq \underbrace{\left(P_0^{\frac{1}{p}} + \mathbb{E}_{\mu_{N_m}} [|N_m|^p]^{\frac{1}{p}} \right)^p}_{\hat{U}_0}. \end{aligned} \quad (64)$$

Consequently, (61) can be further written as

$$C \leq \inf_{\sigma_1} \left\{ -\log \frac{p}{2\Gamma(1/p)} + \underbrace{\frac{1}{p} \log \sigma_1 + \frac{\hat{U}_0}{\sigma_1}}_{\hat{U}_1(\sigma_1)} - h(N_m) \right\}. \quad (65)$$

The best σ_1 can be determined from the first derivative of $\hat{U}_1(\sigma_1)$. Notice that \hat{U}_0 is not related with σ_1 ,

$$\frac{\partial \hat{U}_1(\sigma_1)}{\partial \sigma_1} \Big|_{\sigma_1=\sigma_1^*} = 0 \Rightarrow \sigma_1^* = p\hat{U}_0. \quad (66)$$

After some substitutions and simplifications, the first capacity upper bound will be (60). ■

2) *Asymptotical behaviors and generality*: With the similar analysis of the asymptotic behavior of lower bounds, U can also converge to Shannon formula when MGIN degenerates to WGN. In the next, we discuss the asymptotic relation between L_2 and U since the input distribution for L_2 and the output distribution for U are the same. We first denote the difference

$$\Delta B \triangleq U - L_2 > 0. \quad (67)$$

As the P_0 continuously increases such that $P_0 \gg \mathbb{E}_{\mu_{N_m}}[|N_m|^p]$, we have

$$\begin{aligned} \Delta B &\approx U - \frac{1}{2} \log \left(1 + e^{2[1/p - \lambda_0 - h(N_m)]} \right) \\ &= -\log \frac{p}{2\Gamma(1/p)} + \frac{1}{p} \log P_0 + \frac{1}{p} \log p + \frac{1}{p} \\ &\quad - \frac{1}{2} \log \left(1 + e^{2[1/p - \lambda_0 - h(N_m)]} \right). \end{aligned} \quad (68)$$

According to the (49), $-\lambda_0$ is also quite large. Consequently,

$$\begin{aligned} \Delta B &\approx -\log \frac{p}{2\Gamma(1/p)} + \frac{1}{p} \log P_0 + \frac{1}{p} \log p + \frac{1}{p} \\ &\quad - \left(\frac{1}{p} - \lambda_0 - h(N_m) \right) \triangleq \Delta B(P_0). \end{aligned} \quad (69)$$

With some simplifications, we have $\lim_{P_0 \rightarrow +\infty} \Delta B(P_0) = 0$. Therefore, L_2 and U converge to the same value when the input power is large enough. Furthermore, we can also obtain the asymptotic channel capacity expression under the constraints (17) and (18) as follows,

$$\lim_{P_0 \rightarrow +\infty} C(p, P_0) = -\log \frac{p}{2\Gamma(1/p)} + \frac{\log(pP_0) + 1}{p} - h(N_m), \quad (70)$$

where $1 \leq p < \alpha \leq 2$. Then, we consider the case that $\alpha \rightarrow 2$ to verify the correctness and generality of (70). In fact, when the input signal power is large enough,

$$\begin{aligned} \lim_{\alpha \rightarrow 2} C(2, P_0) &\approx \log \Gamma(1/2) + \frac{\log(2eP_0)}{2} - \lim_{\alpha \rightarrow 2} h(N_m) \\ &\approx \frac{1}{2} \log(2\pi e P_0) - \frac{1}{2} \log(4\pi e \gamma_{nsg}) \\ &= \frac{1}{2} \log \left(\frac{P_0}{2\gamma_{nsg}} \right). \end{aligned} \quad (71)$$

According to (3), when $\alpha = 2$ and $c_1 = 1$, $2\gamma_{nsg}$ is equivalent to the noise variance and represents the power of noise. Thus,

$$\lim_{\alpha \rightarrow 2} C(2, P_0) = \lim_{P_0 \rightarrow +\infty} \frac{1}{2} \log \left(\frac{P_0}{P_N} \right), \quad (72)$$

where P_N denotes the noise power. It can be seen that (72) is the same as the Shannon formula when $P_0 \rightarrow +\infty$, which showcases the generality of (70).

Remarks: According to the theorem 2, the choice of p is also related to the tightness of the capacity upper bounds. However, the expression with respect to p is very complicated and the numerical method needs to be applied to determine the optimal p , which is time-consuming. Therefore, we do not consider its optimization and the influence of different p on the bounds will be demonstrated by experimental results.

V. CAPACITY RELATING TO MODULATION SCHEME

In practice, it is valuable to discuss the achievable channel capacity with regard to specific modulation schemes. In this section, we further consider the capacity of M -ary pulse amplitude modulation (M-PAM) under additive MGIN. Note that the M^2 -ary QAM constellation can be considered as two symmetric M-PAM modulated constellations. For instance, We have $C_{16\text{QAM}} = 2C_{4\text{PAM}}$ and consequently, we take the capacity of M-PAM modulation as an example in what follows. We can still employ the BA algorithm to obtain the corresponding capacity. To facilitate application, we derive concise bounds with closed-form expressions. We only consider the lower bound herein based on mutual information function and the upper bound can be also established via relative entropy in Section IV.

Then, we will analyze the relation between power ratio of WGN and IN and the channel capacity. Intuitively, the channel capacity is larger if the WGN takes a larger ratio in the mixed noise. We will verify the conclusion from a new aspect based on the correlation between error probability and mutual information.

A. Lower bounds

First, the mutual information can be expressed as

$$I(P_X) = - \int_{-\infty}^{+\infty} f_Y(y) \log f_Y(y) dy - h(N_m), \quad (73)$$

where P_X denotes the probability mass function (PMF) of X . $f_Y(y)$ is

$$f_Y(y) = \sum_{j=1}^M p(x_j) f_{N_m}(y|x=x_j), \quad (74)$$

where M is the modulation order. (73) can not be expressed with closed-form due to the complexity of $f_Y(y)$. Therefore, we will resort to Gauss-Hermite quadrature (GHQ) to approximate (73) by a finite sum. $h(N_m)$ is independent of the input distribution and is calculated in Appendix A. $h(Y)$ is expressed as

$$\begin{aligned} h(Y) &= - \int_{-\infty}^{+\infty} f_Y(y) \log f_Y(y) dy \\ &\geq - \log \int_{-\infty}^{+\infty} [f_Y(y)]^2 dy, \end{aligned} \quad (75)$$

where (75) follows Jensen inequality. If the number of the polynomial terms is adequate, the GHQ can be an accurate estimation of infinite integral with the following form,

$$\int_{-\infty}^{+\infty} e^{-x^2} f(x) dx \approx \sum_{j=0}^{N_h} A_j f(\bar{x}_j), \quad (76)$$

where A_j is the weight factors, N_h is the order of polynomials and \bar{x}_j is the zeros of Hermite polynomials which is symmetric about 0 [22]. Note that if function $f(x)$ could not satisfy (76), it can be transformed as follows,

$$\int_{-\infty}^{+\infty} f(x) dx = \int_{-\infty}^{+\infty} e^{-x^2} [e^{x^2} f(x)] dx. \quad (77)$$

Thus, we can also simplify $I(P_X)$ to

$$I(P_X) \geq -\log \left\{ \sum_{j=0}^N e^{\bar{x}_j^2} [f_Y(\bar{x}_j)]^2 \right\} - h(N_m) \triangleq \hat{L}_1. \quad (78)$$

Besides, we can also utilize Fano inequality to obtain the lower bound of (73). First, we define a RV V with the PMF to be $f_V(v) = P_e \delta(v) + (1 - P_e) \delta(v - 1)$ where P_e is the symbol error rate of 4-PAM. Then, Fano inequality is expressed as [6]

$$h(X|Y) \leq h(V) + P_e \log(|X| - 1), \quad (79)$$

where $|X|$ represents the cardinality of feasible set of X . Without loss of generality, we can set the input distribution of M-PAM to be uniform in both probability and space to get a lower bound conveniently. Consequently, based on (8) and (9), P_e for the mixed noise channel is

$$\begin{aligned} P_e &= \frac{2(M-1)}{M} \int_{\frac{A}{2}}^{+\infty} f_{N_m}(n) dn \\ &= \frac{2(M-1)g_0}{MI} \left[c_1 \int_{\frac{A}{2}}^{+\infty} e^{-\frac{n^2}{4\gamma_{sg}}} dn + c_2(1 - c_1) \right. \\ &\quad \times \left. \int_{\frac{A}{2}}^{+\infty} \frac{dn}{n^{\alpha+1} + c_2} \right] \\ &= \frac{2(M-1)g_0}{MI} \left\{ c_1 \sqrt{\pi\gamma_{sg}} \mathcal{Q} \left(\frac{A}{2\sqrt{2\gamma_{sg}}} \right) + (1 - c_1) \right. \\ &\quad \times \left[c_2^{\frac{1}{\alpha+1}} \Gamma \left(\frac{\alpha+2}{\alpha+1} \right) \Gamma \left(\frac{\alpha}{\alpha+1} \right) - \frac{A}{2} \right. \\ &\quad \times \left. \left. {}_2F_1 \left(1, \frac{1}{\alpha+1}; \frac{\alpha+2}{\alpha+1}; -\frac{A^{\alpha+1}}{c_2^{\alpha+1}} \right) \right] \right\}, \quad (80) \end{aligned}$$

where A represents the distance of two adjacent constellation points. Considering the power constraint jointly, we can get that

$$2 \sum_{j=1}^{M/2} \left[\frac{A}{2} (2j-1) \right]^p = P_0, \quad (81)$$

and

$$A = 2 \left[\frac{P_0}{2 \sum_{j=1}^{M/2} (2j-1)^p} \right]^{\frac{1}{p}}. \quad (82)$$

Finally, the mutual information can be expressed as

$$\begin{aligned} I(P_X) &= h(X) - h(X|Y) \\ &\geq \log M - h(V) - P_e \log(M-1) \\ &= \log M + P_e \log \frac{P_e}{M-1} + (1 - P_e) \log(1 - P_e) \\ &\triangleq \hat{L}_2. \end{aligned} \quad (83)$$

Plugging (80) into (83), we can get the second lower bound \hat{L}_2 . The effectiveness of \hat{L}_1 and \hat{L}_2 will be discussed in the next section.

B. Influence of the ratio of WGN in the mixed noise

For the equiprobable binary input memoryless channel, the upper bound of the maximum likelihood (ML) detection error probability is defined by the Bhattacharyya parameter, i.e.,

$$Z(W) = \int_Y \sqrt{W(y|0)W(y|A)} dy. \quad (84)$$

For simplicity, we utilize $I(W)$ to denote the mutual information of the mixed noise channel with equiprobable binary input. In [23], it is shown that

$$I(W) \leq \sqrt{1 - Z(W)^2}. \quad (85)$$

The detection error probability has been given in (80) and it is related c_1 which is the ratio of WGN and IN. We consider the high GSNR regime in which case the signal amplitude A is relatively large. Then, the $\mathcal{Q}(A/2\sqrt{2\gamma_{sg}})$ is very small compared with the remaining part. Therefore, when the c_1 is small, the P_e becomes larger. As the upper bound of P_e , $Z(W)$ is larger and based on (85), the upper bound of the mutual information is smaller. Consequently, the channel capacity also decreases with smaller c_1 or equivalently, a larger power ratio of IN in the mixed noise. The analysis can also be applied to demonstrate that the capacity of pure IN channel is lower than that of the WGN case.

VI. NUMERICAL RESULTS

In this section, we present numerical results to validate the analysis in this paper. We will first calculate the numerical channel capacity of the mixed noise in various scenarios. Then, the bounds and capacity comparisons with different α and p are performed to validate the tightness of our bounds. Finally, we consider the practical application of the channel capacity with 4-PAM modulation. Due to the lack of finite variance, we first define the generalized signal-to-noise ratio (GSNR) to be

$$\text{GSNR(dB)} = 10 \log_{10} \frac{\mathbb{E}_{\mu_X} [|X|^p]}{\mathbb{E}_{\mu_{N_m}} [|N_m|^p]}, \quad (86)$$

where $0 < p \leq \alpha$. As the capacity curves corresponding to different p have different slopes, we set $p = \min\{I_\alpha\} - 0.1$ where I_α is the set containing all α used in simulation. As for the capacity bounds, we also consider the influence of different p on the tightness of bounds with a fixed α .

A. Numerical Capacity

We leverage BA algorithm to compute the capacity numerically. To adopt the BA algorithm, we need to discretize and truncate the mixed noise model. To decrease the error, the truncation point n_T should be as large as possible. We set the range of n in $f_{N_m}(n)$ to be $|n| \leq n_T$ and $n_T = \min\{n_r : \int_{-n_r}^{n_r} f_{N_m}(n)dn > 0.999\}$. Note that n_T will increase rapidly when both α and GSNR are quite small, in which case the resolution of the horizontal axis should be larger to pursue less computational complexity. However, when the GSNR becomes very large, the whole PDF will concentrate in a rather limited range and the resolution needs to increase. Thus, the trade-off of the horizontal axis step is set to 0.01 to assure the accuracy of the model.

Meanwhile, we also verify the generality of results when the channel degenerates to a pure impulsive channel and Gaussian channel. The numerical capacities for different α are shown in Fig. 1. ‘ $\alpha = 1.2$ (pure)’ represents that the noise is pure IN with $\alpha = 1.2$. It can be seen that the capacity becomes larger when α is closer to 2 and the Gaussian noise channel has the largest capacity. The capacity of S α S distributed pure impulsive noise channel is the smallest one, which verifies that the channel capacity decreases when the impulsiveness of noise is more considerable. Note that there is an obvious capacity gap between the ‘ $\alpha = 1.2$ ’ and ‘ $\alpha = 1.2$ (pure)’. The gap is about 1dB when they have the same capacity, which indicates that the power ratio of WGN in the mixed noise has a considerable influence on the channel capacity.

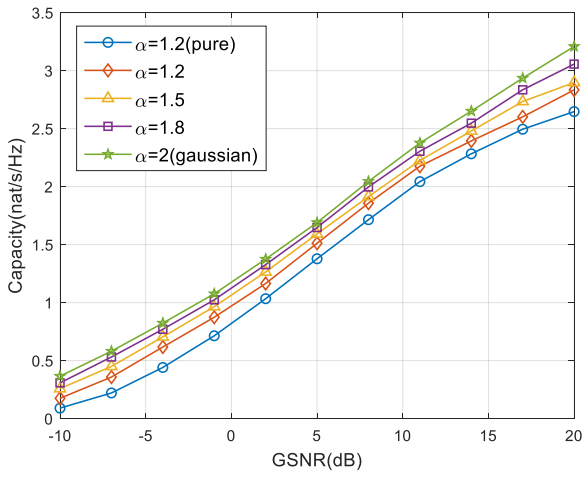


Fig. 1. Numerical capacity with different values of α and $p = 1.1$

B. Comparison of Capacity and Bounds

In this subsection, we investigate the capacity bounds with different α and p . We choose $\alpha = 1.2$ and $\alpha = 1.9$ to represent different impulsiveness. The mixed noise channel with $\alpha = 1.9$ is close to WGN, which has a larger capacity.

The capacities and bounds are shown in Fig. 2-4. In general, the lower bound L_2 and the upper bound U are quite tight in various scenarios especially when α is larger for a given p . Meanwhile, L_2 and U are asymptotic and converge to the

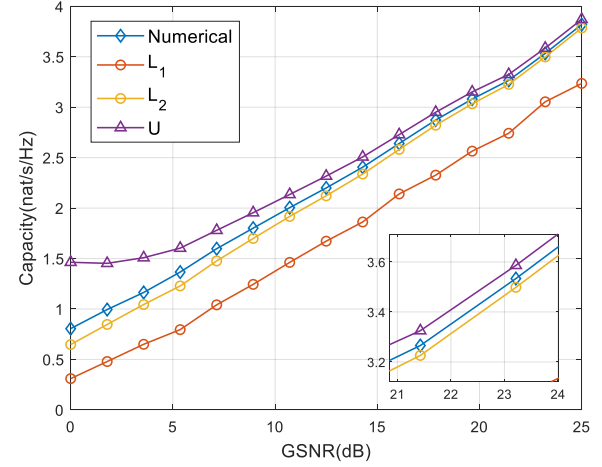


Fig. 2. Capacity and bounds with $\alpha = 1.2, p = 1.1$

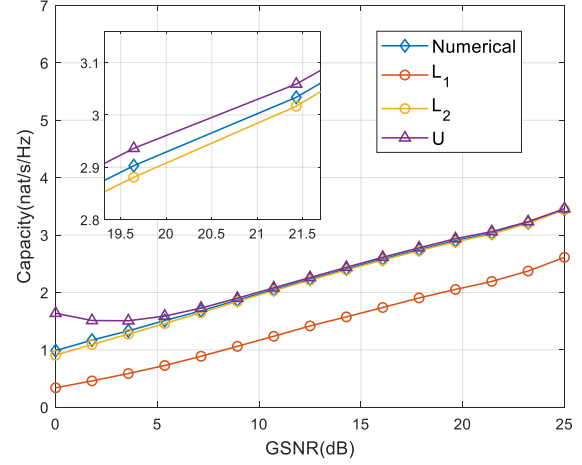


Fig. 3. Capacity and bounds with $\alpha = 1.9, p = 1.1$

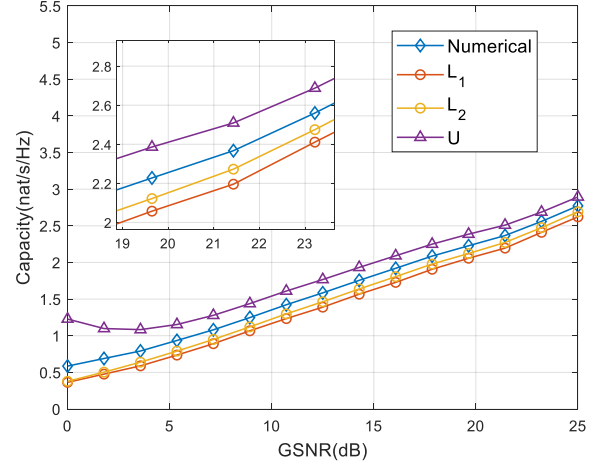


Fig. 4. Capacity and bounds with $\alpha = 1.9, p = 1.8$

numerical capacity as GSNR increases. L_1 is less tight and there is an obvious gap between the bounds and the capacity, which demonstrates that the optimal input distribution is not heavy-tail. From Fig. 4, it can be expected that the lower bound L_1 is also tighter as α becomes larger and coincides with the channel capacity for $\alpha = 2$ since the corresponding input and output distributions are both optimal, i.e., Gaussian distribution. As the upper bounds are not monotonic and convex functions, they decrease as GSNR increases in the low GSNR region.

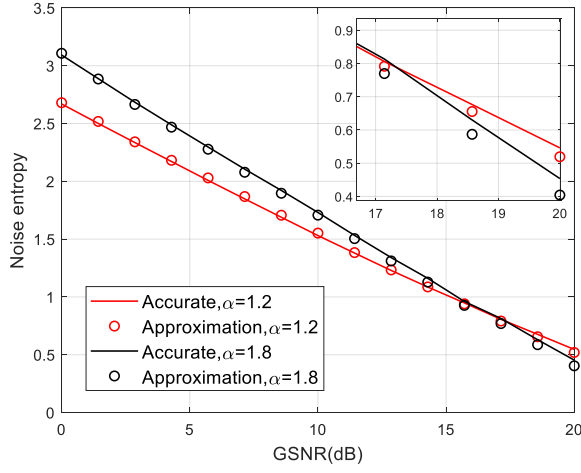


Fig. 5. The comparison of noise entropy based on (3) and (41) with different α

In addition, we provide the comparison of the noise entropy calculated by the mixed noise model in (3) and the approximated model in (41) since the analytical noise entropy expression is obtained based on (41). The result is presented in Fig. 5. It can be seen that the approximation matches the ground truth very well in the whole GSNR region. The largest entropy difference happens at $\alpha = 1.8$ and GSNR = 20dB. The reason is that the noise PDF concentrates at the origin and the intersection point n_0 in the theorem 1 is close to 0 with a large GSNR. Thus, the estimated n_0 is less accurate with the fixed scale of the horizontal step if the GSNR becomes larger. In other words, the difference can be smaller if the horizontal step continues to decrease. Therefore, the simplified noise model can be utilized to derive the capacity bounds and the noise entropy expression in Appendix A is accurate enough.

C. Capacity and bound under 4-PAM Modulation

The capacity under modulation order constraint with different α is shown in Fig. 6. Compared with the results presented in Fig. 1, the capacity upper limit can be observed since a symbol under 4-PAM modulation can represent at most 2 bits. Similar to the channel capacity without modulation order constraint, to reach the same bit error rate (BER) performance, the smaller α is, the larger the required GSNR is. The capacity with various α will be 2 bit/s/Hz when GSNR $\rightarrow +\infty$. However, the capacity becomes stable when GSNR is larger than 25dB, which implies that the capacity improvement for

communication systems is slight via increasing the GSNR if it is large enough.

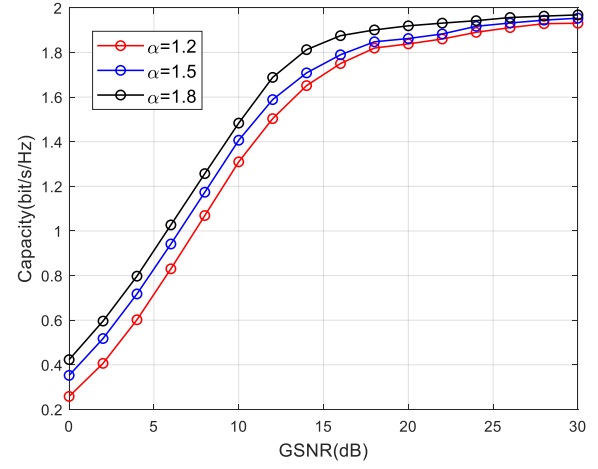
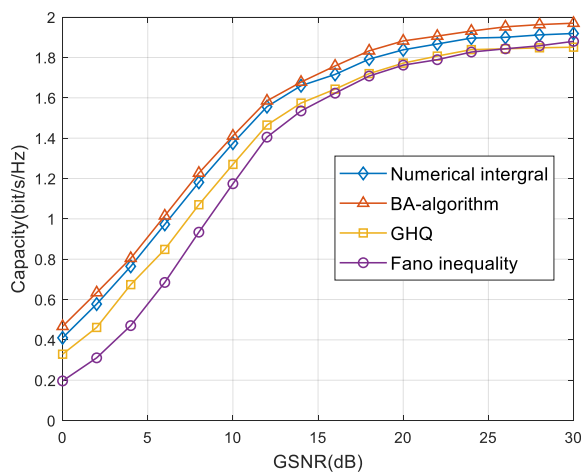


Fig. 6. Capacity of 4-PAM with different α

Finally, the capacity and its lower bounds are verified in Fig. 7. To assure the accuracy of GHQ, we choose the order of polynomials N_h to be 30. The ‘BA algorithm’ and ‘Numerical integral’ denote the numerical capacity calculated by BA algorithm and the capacity when the input is equiprobable and equispaced, respectively. Note that the number of polynomial terms N_h used in GHQ increases when GSNR becomes too large, e.g., 30dB. In that case, $f_Y(y)$ is similar to the linear combination of the delta function which makes it difficult for GHQ to produce a reasonable estimation. For instance, to retain the estimation accuracy, we need to have $N_h \geq 50$ if GSNR continues to increase. The bound based on Fano’s inequality is more accurate when GSNR is larger and P_e is smaller. Note that when $P_e \rightarrow 0$, \hat{L}_2 becomes $\log M$ which is the capacity limit of M-PAM. In other words, the bound in (83) can converge to capacity when GSNR is large enough. Moreover, the results demonstrate that the mutual information is rather close to the capacity, especially when GSNR is relatively large. It means that the equiprobable and equispaced constellation is an effective choice in the MGIN channel.

VII. CONCLUSION

In this paper, we systematically analyzed the capacity and capacity bounds of the MGIN channel. The MGIN channel model and some pertinent properties were first given. Then, we theoretically showed the existence and uniqueness of the capacity. For practical applications, concise and closed-form lower and upper bounds of the capacity were given. Theoretical analysis showcased that the lower bounds can degrade to Shannon formula when MGIN becomes WGN and we obtained the asymptotic capacity expression with the closed form. We also considered the capacity for 4-PAM modulation scheme under MGIN channel and proposed two lower bounds. Experimental results verified that the capacity is related to α , and our bounds were tight particularly when α and GSNR are large.

Fig. 7. Capacity and lower bounds of 4-PAM with $\alpha = 1.5$

APPENDIX A DERIVATION OF L_1

Before starting the derivation of L_1 , we first provide two integral formulas that will be used in the following [19],

$$\int \frac{(x-c)^p}{x} dx = \frac{x^p}{c} {}_2F_1 \left(-p, -p; 1-p; -\frac{x}{c} \right), \quad (\text{A.1})$$

$$\int x^p {}_2F_1 (a, b; c; x) dx = \frac{x^{p+1}}{p+1} {}_3F_2 (a, b, p+1; c, p+2; x), \quad (\text{A.2})$$

where ${}_pF_q (\cdot)$ is the generalized hypergeometric function.

The capacity is lower bounded by mutual information, i.e., $C \geq I(F_X) = h(Y) - h(N_m)$. Note that we only need to calculate $h(Y)$ as both Y and N_m follow the mixed noise model with the same α . It follows the theorem 1 that $h(Y)$ can be expressed as

$$\begin{aligned} h(Y) &\approx -2 \int_0^{+\infty} \hat{f}_{N_m}(y) \log \hat{f}_{N_m}(y) dy \\ &= -2 \int_0^{y_0} \frac{g_{y0}}{I_y} e^{-\frac{y^2}{4\gamma_{ysg}}} \log \frac{g_{y0}}{I_y} e^{-\frac{y^2}{4\gamma_{ysg}}} dy \\ &\quad - 2 \underbrace{\int_{y_0}^{+\infty} \frac{\alpha \gamma_{ys} C_\alpha}{I_y (y^{\alpha+1} + c_{y2})} \log \frac{\alpha \gamma_{ys} C_\alpha}{I_y (y^{\alpha+1} + c_{y2})} dy}_{L_1^*}. \end{aligned} \quad (\text{A.3})$$

The first term of (A.3) is easier to calculate, i.e.,

$$\begin{aligned} &- \frac{2g_{y0}}{I_y} \int_0^{y_0} \left(\log \frac{g_{y0}}{I_y} - \frac{y^2}{4\gamma_{ysg}} \right) e^{-\frac{y^2}{4\gamma_{ysg}}} dy \\ &= - \frac{g_{y0}}{I_y} \left\{ y_0 e^{-\frac{y_0^2}{4\gamma_{ysg}}} + \left(2 \log \frac{g_{y0}}{I_y} - 1 \right) \sqrt{\pi \gamma_{ysg}} \right. \\ &\quad \left. \times \left[1 - 2\mathcal{Q} \left(\frac{y_0}{\sqrt{2\gamma_{ysg}}} \right) \right] \right\}. \end{aligned} \quad (\text{A.4})$$

Note that C_α is only related with α . The L_1^* admits closed-form expression by (A.1) and (A.2). We first divide it into two parts,

$$\begin{aligned} L_1^* &= \int_{y_0}^{+\infty} \frac{\alpha \gamma_{ys} C_\alpha}{I_y (y^{\alpha+1} + c_{y2})} \log \left(\frac{\alpha \gamma_{ys} C_\alpha}{I_y} \right) dy \\ &\quad - \underbrace{\int_{y_0}^{+\infty} \frac{\alpha \gamma_{ys} C_\alpha}{I_y (y^{\alpha+1} + c_{y2})} \log (y^{\alpha+1} + c_{y2}) dy}_{L_1^{**}} \\ &= \frac{\alpha \gamma_{ys} C_\alpha}{I_y c_{y2}} \log \left(\frac{\alpha \gamma_{ys} C_\alpha}{I_y} \right) \left[c_{y2}^{\frac{1}{\alpha+1}} \Gamma \left(\frac{\alpha}{\alpha+1} \right) \Gamma \left(\frac{\alpha+2}{\alpha+1} \right) \right. \\ &\quad \left. - 2F_1 \left(1, \frac{1}{\alpha+1}; \frac{\alpha+2}{\alpha+1}; -\frac{y_0^{\alpha+1}}{c_{y2}} \right) y_0 \right] - L_1^{**}. \end{aligned} \quad (\text{A.5})$$

The last equation follows the formula (8). Let $u = y^{\alpha+1} + c_{y2}$, L_1^{**} can then be represented as

$$L_1^{**} = \frac{\alpha \gamma_{ys} C_\alpha}{I_y (\alpha+1)} \int_{\kappa_y}^{+\infty} (u - c_{y2})^{-\frac{\alpha}{\alpha+1}} \frac{\log u}{u} du, \quad (\text{A.6})$$

where we denote $\kappa_y = y_0^{\alpha+1} + c_{y2}$. Then, L_1^{**} becomes (87) based on the partial integration. The second equation is gotten by the variable transform $u \triangleq t^{-1}$ and follows the integral formula (A.1).

According to (A.2), L^\dagger can be expressed as

$$\begin{aligned} L^\dagger &= {}_3F_2 \left(\frac{\alpha}{\alpha+1}, \frac{\alpha}{\alpha+1}, \frac{\alpha}{\alpha+1}; \frac{2\alpha+1}{\alpha+1}, \frac{2\alpha+1}{\alpha+1}; \frac{c_{y2}}{\kappa_y} \right) \\ &\quad \times \frac{\alpha+1}{\alpha} \kappa_y^{-\frac{\alpha}{\alpha+1}}. \end{aligned} \quad (\text{A.7})$$

Finally, combining (A.3), (87) and (A.7), $h(Y)$ is shown in (88). Note that the expression is a little complicated but it is analytic. Meanwhile, $h(N_m)$ could be similarly expressed by substituting the corresponding parameters. Then, we can obtain the lower bound in (44).

REFERENCES

- [1] U. Epple and M. Schnell, "Advanced blanking nonlinearity for mitigating impulsive interference in ofdm systems," *IEEE Trans. Veh. Technol.*, vol. 66, no. 1, pp. 146–158, 2017.
- [2] P. Chen, Y. Rong, S. Nordholm, Z. He, and A. J. Duncan, "Joint channel estimation and impulsive noise mitigation in underwater acoustic ofdm communication systems," *IEEE Trans. Wireless Commun.*, vol. 16, no. 9, pp. 6165–6178, 2017.
- [3] M. Zimmermann and K. Dostert, "Analysis and modeling of impulsive noise in broad-band powerline communications," *IEEE Trans. Electromagn. Compat.*, vol. 44, no. 1, pp. 249–258, 2002.
- [4] M. Shao and C. Nikias, "Signal processing with fractional lower order moments: stable processes and their applications," *Proc. IEEE Proc. IRE**, vol. 81, no. 7, pp. 986–1010, 1993.
- [5] T. Qi, J. Wang, X. Chen, W. Huang, and Q. Peng, "Capacity of the mixed gaussian-impulsive noise channel," in *2023 IEEE 98th Vehicular Technology Conference (VTC2023-Fall)*, 2023, pp. 1–5.
- [6] T. M. Cover and J. A. Thomas, *Elements of Information Theory*. John Wiley & Sons, Ltd, 2005. [Online]. Available: <https://onlinelibrary.wiley.com/doi/pdf/10.1002/047174882X.ch4>
- [7] I. Abou-Faycal, M. Trott, and S. Shamai, "The capacity of discrete-time memoryless rayleigh-fading channels," *IEEE Trans. Inf. Theory*, vol. 47, no. 4, pp. 1290–1301, 2001.
- [8] H. Li, S. M. Moser, and D. Guo, "Capacity of the memoryless additive inverse gaussian noise channel," *IEEE J. Sel. Areas Commun.*, vol. 32, no. 12, pp. 2315–2329, 2014.
- [9] A. Lapidot and S. Moser, "Capacity bounds via duality with applications to multiple-antenna systems on flat-fading channels," *IEEE Trans. Inf. Theory*, vol. 49, no. 10, pp. 2426–2467, 2003.

$$\begin{aligned}
& \int_{\kappa_y}^{+\infty} (u - c_{y2})^{-\frac{\alpha}{\alpha+1}} \frac{\log u}{u} du \\
&= \frac{\alpha+1}{\alpha} \left[\frac{\log \kappa_y}{\kappa_y^{\frac{\alpha}{\alpha+1}}} {}_2F_1 \left(\frac{\alpha}{\alpha+1}, \frac{\alpha}{\alpha+1}; 1 + \frac{\alpha}{\alpha+1}; \frac{c_{y2}}{\kappa_y} \right) + \underbrace{\int_0^{\kappa_y^{-1}} t^{\frac{-1}{\alpha+1}} {}_2F_1 \left(\frac{\alpha}{\alpha+1}, \frac{\alpha}{\alpha+1}; 1 + \frac{\alpha}{\alpha+1}; c_{y2}t \right) dt}_{L^\dagger} \right]. \quad (87)
\end{aligned}$$

$$\begin{aligned}
h(Y) = & -\frac{g_{y0}}{I_y} \left\{ y_0 e^{-\frac{y_0^2}{4\gamma_{ysg}}} + \left(2 \log \frac{g_{y0}}{I_y} - 1 \right) \sqrt{\pi \gamma_{ysg}} \left[1 - 2Q \left(\frac{y_0}{\sqrt{2\gamma_{ysg}}} \right) \right] \right\} - \frac{2\alpha \gamma_{ys} C_\alpha}{I_y c_{y2}} \log \left(\frac{\alpha \gamma_{ys} C_\alpha}{I_y} \right) \left[c_{y2}^{\frac{1}{\alpha+1}} \Gamma \left(\frac{\alpha}{\alpha+1} \right) \right. \\
& \times \Gamma \left(\frac{\alpha+2}{\alpha+1} \right) - {}_2F_1 \left(1, \frac{1}{\alpha+1}; \frac{\alpha+2}{\alpha+1}; -\frac{y_0^{\alpha+1}}{c_{y2}} \right) y_0 \left. \right] + \frac{2\gamma_{ys} C_\alpha}{I_y} \left[\frac{\log \kappa_y}{\kappa_y^{\frac{\alpha}{\alpha+1}}} {}_2F_1 \left(\frac{\alpha}{\alpha+1}, \frac{\alpha}{\alpha+1}; 1 + \frac{\alpha}{\alpha+1}; \frac{c_{y2}}{\kappa_y} \right) \right. \\
& + {}_3F_2 \left(\frac{\alpha}{\alpha+1}, \frac{\alpha}{\alpha+1}, \frac{\alpha}{\alpha+1}; \frac{2\alpha+1}{\alpha+1}, \frac{2\alpha+1}{\alpha+1}; \frac{c_{y2}}{\kappa_y} \right) \frac{\alpha+1}{\alpha} \kappa_y^{-\frac{\alpha}{\alpha+1}} \left. \right]. \quad (88)
\end{aligned}$$

- [10] A. Lapidoth, S. M. Moser, and M. A. Wigger, "On the capacity of free-space optical intensity channels," *IEEE Trans. Inf. Theory*, vol. 55, no. 10, pp. 4449–4461, 2009.
- [11] A. Lapidoth, J. H. Shapiro, V. Venkatesan, and L. Wang, "The discrete-time poisson channel at low input powers," *IEEE Trans. Inf. Theory*, vol. 57, no. 6, pp. 3260–3272, 2011.
- [12] J. Wang, E. E. Kuruglu, and T. Zhou, "Alpha-stable channel capacity," *IEEE Commun. Lett.*, vol. 15, no. 10, pp. 1107–1109, 2011.
- [13] M. L. de Freitas, M. Egan, L. Clavier, A. Goupil, G. W. Peters, and N. Azaoui, "Capacity bounds for additive symmetric α -stable noise channels," *IEEE Trans. Inf. Theory*, vol. 63, no. 8, pp. 5115–5123, 2017.
- [14] M. He, S. Lu, G. Song, J. Cheng, and Y. Watanabe, "Channel capacity with superposed m-pam modulation," in *2011 Fourth International Conference on Intelligent Computation Technology and Automation*, vol. 2, 2011, pp. 475–478.
- [15] G. Cai, L. Wang, and T. Huang, "Channel capacity of m-ary differential chaos shift keying modulation over awgn channel," in *2013 13th International Symposium on Communications and Information Technologies (ISCIT)*, 2013, pp. 91–95.
- [16] P. Yang, Y. Wu, and H. Yang, "Capacity of nakagami- m fading channel with bpsk/qpsk modulations," *IEEE Commun. Lett.*, vol. 21, no. 3, pp. 564–567, 2017.
- [17] G. Sureka and K. Kiasaleh, "Sub-optimum receiver architecture for awgn channel with symmetric alpha-stable interference," *IEEE Trans. Commun.*, vol. 61, no. 5, pp. 1926–1935, 2013.
- [18] G. Samorodnitsky and M. S. Taqqu, *Stable Non-Gaussian Random Processes: Stochastic Models with Infinite Variance*. New York: Chapman & Hall, 1994.
- [19] D. Zwillinger, V. Moll, I. Gradshteyn, and I. Ryzhik, Eds., *Table of Integrals, Series, and Products (Eighth Edition)*. Boston: Academic Press, 2014.
- [20] S. Boyd and L. Vandenberghe, *Convex Optimization*. Cambridge: Cambridge University Press, 2004.
- [21] J. Fahs and I. Abou-Faycal, "On properties of the support of capacity-achieving distributions for additive noise channel models with input cost constraints," *IEEE Trans. Inf. Theory*, vol. 64, no. 2, pp. 1178–1198, 2018.
- [22] F. Olver, D. Lozier, R. Boisvert, and C. Clark, *NIST Handbook of Mathematical Functions*. New York: Cambridge University Press, 2010.
- [23] E. Arikan, "Channel polarization: A method for constructing capacity-achieving codes for symmetric binary-input memoryless channels," *IEEE Trans. Inf. Theory*, vol. 55, no. 7, pp. 3051–3073, 2009.